NRL Memorandum Report 4112

Computer Simulation of Gradient Drift Instability Processes in Operation Avefria

B. E. McDonald, M. J. Keskinen, S. L. Ossakow, and S. T. Zalesak

Geophysical and Plasma Dynamics Branch
Plasma Physics Division

November 15, 1979

This research was sponsored by the Defense Nuclear Agency under Subtask S99QAXHC041, work unit 12 and work unit title Ionization Structured Research.

NAVAL RESEARCH LABORATORY
Washington, D.C.

Approved for public release; distribution unlimited.

ADA077668

SECURITY CLASSIFICATION OF THIS PAGE *(When Date Entered)*

REPORT DOCUMENTATION PAGE		READ INSTRUCTIONS BEFORE COMPLETING FORM
1. REPORT NUMBER NRL Memorandum Report 4112	2. GOVT ACCESSION NO.	3. RECIPIENT'S CATALOG NUMBER
4. TITLE *(and Subtitle)* COMPUTER SIMULATION OF GRADIENT DRIFT INSTABILITY PROCESSES IN OPERATION AVEFRIA		5. TYPE OF REPORT & PERIOD COVERED Interim report on a continuing NRL problem. 6. PERFORMING ORG. REPORT NUMBER
7. AUTHOR(s) B. E. McDonald, M. J. Keskinen*, S. L. Ossakow and S. T. Zalesak		8. CONTRACT OR GRANT NUMBER(s)
9. PERFORMING ORGANIZATION NAME AND ADDRESS Naval Research Laboratory Washington, DC 20375		10. PROGRAM ELEMENT, PROJECT, TASK AREA & WORK UNIT NUMBERS NRL Problem 67H02-27B DNA Subtask S99QAXHC041
11. CONTROLLING OFFICE NAME AND ADDRESS Defense Nuclear Agency Washington, DC 20305		12. REPORT DATE November 15, 1979 13. NUMBER OF PAGES 37
14. MONITORING AGENCY NAME & ADDRESS*(if different from Controlling Office)*		15. SECURITY CLASS. *(of this report)* UNCLASSIFIED 15a. DECLASSIFICATION/DOWNGRADING SCHEDULE

16. DISTRIBUTION STATEMENT *(of this Report)*

Approved for public release; distribution unlimited.

17. DISTRIBUTION STATEMENT *(of the abstract entered in Block 20, if different from Report)*

18. SUPPLEMENTARY NOTES

*NRC/NRL Resident Research Associate

This research was sponsored by the Defense Nuclear Agency under Subtask S99QAXHC041, work unit 12 and work unit title Ionization Structured Research.

19. KEY WORDS *(Continue on reverse side if necessary and identify by block number)*

Gradient drift instability
Operation Avefria
Physically small plasma clouds
Nonlinear computer simulation
Striations

20. ABSTRACT *(Continue on reverse side if necessary and identify by block number)*

We have solved numerically equations of motion for the evolution of a one level, two dimensional F region ionospheric plasma cloud with five different ratios of cloud to background integrated Pedersen conductivity. The simulations show that (1) physically small clouds striate due to the gradient drift instability more rapidly than large clouds, and (2) there exists a minimum striation onset time as a function of the Pedersen conductivity ratio. Observation (1) is in agreement with the rapid striation development exhibited by the physically small Avefria barium cloud releases, relative to the large Secede or STRESS type releases.

DD FORM 1 JAN 73 1473 EDITION OF 1 NOV 65 IS OBSOLETE
S/N 0102-014-6601

SECURITY CLASSIFICATION OF THIS PAGE *(When Date Entered)*

CONTENTS

COMPUTER SIMULATION OF GRADIENT DRIFT INSTABILITY PROCESSES IN OPERATION AVEFRIA

1. INTRODUCTION

During May 6-20, 1978, Pongratz et al. (1978) conducted two barium release experiments (Avefria Uno and Dos) near Tonopah, Nevada. Shaped-charged releases of 1.45 kg of metallic barium were detonated at an altitude of 192 km, approximately 40 minutes before sunrise. One of the goals of the experiment was to study effects of the highly directed jet of barium ions created by the detonation. Irregularities produced at some distance from the explosion by the jet were visible within 5-10 seconds of the detonation (see Figure 1). These were probably due to kinetic instabilities, and will not be considered here. However, in the vicinity of the detonation, a plasma cloud of roughly spherical shape developed striations of the gradient-drift type (Figs. 2-5). The spatial and temporal evolution of these striations was noticably different from that observed in larger barium releases. The onset of striations in the Avefria Dos cloud occurred 135 seconds after detonation, as opposed to times greater than approximately 300 seconds for larger barium clouds (Davis et al., 1974). The Avefria Dos cloud attained what might be called a "fully developed state" approximately 3 minutes after detonation, as opposed to 15 to 20 minutes for the larger earlier releases (Davis et al., 1974). The structures emerging from the spherical portion of the cloud, as shown in Figs. 4 and 5 are to be contrasted

Note: Manuscript submitted September 17, 1979.

with those seen in previous releases. The structures of Figs. 4 and 5 are more amorphous or inkblot-like than the long, parallel finger striations typical of larger releases (e.g., Spruce, from Secede barium series, Fig. 6).

We believe that the rapid development of Avefria gradient drift striations was due to its physical smallness (~1 km initial radius as opposed to approximately 5 km for Spruce). For example, a linear analysis of the gradient drift instability predicts the linear growth rate γ is proportional to L^{-1}, where L is the cloud plasma density gradient scale length. Consequently, all other things being equal, physically small clouds grow faster according to linear theory. The shape of the Avefria striations may reflect a different ratio of cloud-to-background conductivity than that of earlier releases. These points will be investigated by means of a one-level fluid model to be described below. We feel the use of a one-level model to be justified by the absence of a consistent non zero angle between the striation axes and the neutral wind (Scannapieco, et al., 1974). The direction of the neutral wind relative to the plasma can be determined unambiguously from color photographs showing the drift of the neutral detonation debris cloud away from the plasma cloud. In agreement with linear theory, the neutral wind direction coincides with the direction of initial striation emergence (Fig. 2) (toward the south). The radial arrangement of striations apparent

in Fig. 5 is believed to be a result of parallax and plasma flowing preferentially along the magnetic field. The camera used for Figs. 2-5 was pointed almost directly up the magnetic field. In this paper, section 2 describes the physical equations used, section 3 contains the results from the numerical simulations, and section 4 gives the summary and comparison with the data.

2. EQUATIONS OF MOTION

A few simple arguments will suffice to justify the use of a one-level field-line integrated Pedersen conductivity model to describe the Avefria observations.

For conditions typical of 190 km altitude at sunrise, both electrons and barium ions are magnetized: $\nu_{en}/\Omega_e \approx 2\times10^{-5}$, and $\nu_{in}/\Omega_i \approx 0.04$, where ν_{en} and ν_{in} are respectively the electron and ion collision frequencies with the neutral background; Ω_e and Ω_i are electron and ion gyrofrequencies. For these parameters, the ratio of the cloud's Hall to Pedersen conductivities (Volk and Haerendel, 1971) is approximately ν_{in}/Ω_i, or 0.04. Thus the cloud's field line integrated conductivity is dominated by the Pedersen component. The integrated conductivity of the background ionosphere at twilight is also dominated by the Pedersen component (Francis and Perkins, 1975) with the Hall-to-Pedersen ratio being approximately 1/6. We can estimate the cloud's integrated conductivity as follows. For the parameters given above, the Pedersen conductivity is

$$\sigma_p \approx n \frac{ec}{B} \frac{\nu_{in}}{\Omega_i} , \qquad (1)$$

where n is the ion number density. To obtain an approximate lower limit on n, we assume that only 2% of the barium in the device made up the visible spherical plasma cloud (the pre-launch estimate of Pongratz et al., private communication, 1978, of the fraction of barium vaporized by the detonation and available for ionization was 25%). Taking the cloud to be 1 km in radius, we have $n = 3.0 \times 10^7$ cm^{-3} for the average barium ion density. The estimated cloud-integrated Pedersen conductivity is then the diameter of the cloud times the average conductivity, or $\Sigma_c \approx 8.7$ mho. At the site of the Avefria tests, the integrated Pedersen conductivity of the background ionosphere at twilight (Francis and Perkins, 1975) is $\Sigma_i \approx 3.5$ mho, assuming a magnetic dip angle of 65°. Using 2% and 25% as lower and upper bounds for the fraction of barium atoms ionized and remaining in the spherical portion of the cloud, we find the following lower and upper limits for the ratio of total to background field-line integrated Pedersen conductivity: 3.5/1 and 32/1. Thus the Avefria barium clouds had high enough conductivity that currents may be assumed to close locally, obviating the need for a separate E layer in the model. Two level model numerical simulations (one level for

the plasma cloud and one for the background ionosphere, E or lower F region) of spatially large clouds have been performed (Scannapieco et al., 1976; Doles et al., 1976). However, utilization of a one level model allows for higher numerical simulation resolution than can be attained with two levels.

Justification for a field-line integrated (and thus two dimensional) model comes from the very high conductivity along the field. For the parameter regime

$$\nu_{en}/\Omega_e \ll \min(1, \nu_{in}/\Omega_i) \qquad (2)$$

we have (Volk and Haerendel, 1971)

$$\frac{\sigma_p}{\sigma_\parallel} \approx \frac{\nu_{en}}{\Omega_e} \frac{\nu_{in}\Omega_i}{\nu_{in}^2 + \Omega_i^2}, \qquad (3)$$

where $\sigma_\parallel$ is the conductivity parallel to the magnetic field. This ratio is much less than unity for all parts of the ionosphere, and is of order 2×10^{-6} in the barium cloud. Thus magnetic field lines may be taken to be equipotentials, justifying the use of a field-line integrated continuity equation for n, and thus for the integrated Pedersen conductivity:

$$\Sigma(x,y) \equiv \int \sigma_p(x,y,z)\, dz, \qquad (4)$$

where z is along the magnetic field (curvature of the field lines can be ignored to a high degree of accuracy). The two dimensional (x,y) equations of motion for the one level model are then

$$\frac{\partial \Sigma}{\partial t} = - \nabla \cdot (\Sigma \underline{v}) + \nabla \cdot (K \nabla \Sigma) \qquad (5)$$

$$\underline{v} = - \frac{c}{B} \nabla \phi \times \hat{z} \qquad (6)$$

$$\nabla \cdot (\Sigma \nabla \phi) = \underline{E}_o \cdot \nabla \Sigma \qquad (7)$$

where $\underline{v}$, K, ϕ, B, and $\underline{E}_o$ are respectively the plasma velocity relative to the ambient plasma drift, the cross-field diffusion coefficient, cloud-induced potential, magnetic field strength, and ambient electric field in the neutral rest frame (the electrostatic approximation has been used where $\underline{E} = \underline{E}_o - \nabla \phi$). These equations are adapted from McDonald et al. (1978).

The diffusion coefficient K in (5) is included in the model for the sake of completeness, but for most of the results to be presented here, its effects are small. Using parameter values typical for an altitude of 190km at sunrise, one can approximate the cross-field diffusion coefficient (McDonald et al., 1978) as follows:

$$K \approx K_o \Sigma (x,y)/ \Sigma_i, \quad (8)$$

where $K_o = 1.5 \times 10^4$ cm^2/sec, and $\Sigma_i = 3.5$ mho. This is a rough approximation in two regards: (1) it assumes that a cloud-local diffusion coefficient can be applied to the integrated conductivity; and (2) it assumes the cloud ions diffuse at the same rate as the background ions. On both accounts, (8) is to be regarded as an upper limit on the classical (nonturbulent) cross-field ion diffusion coefficient.

Equations (5) - (7) can be put into nondimensional form (McDonald et al., 1978) to show that cloud evolution depends upon a dimensionless time

$$t' = t \ V/L \quad (9)$$

and an effective Reynolds number

$$R_e = VL/K_o. \quad (10)$$

Here V and L are respectively the plasma drift speed relative to the neutrals and initial gradient scale size. In the simulations to follow, we have chosen V = 100 m/s, and a Gaussian cloud radius of 1 km. Until diffusion effects become important, results from the simulations can be scaled to arbitrary V and L, using (9) to determine t.

3. NUMERICAL SIMULATIONS: A CONDUCTIVITY RATIO STUDY

We have solved numerically eqs. (5) - (7) for five different ratios $M = \Sigma_{max} / \Sigma_i$, where Σ_{max} is the maximum Pedersen conductivity integrated through the center of a Gaussian ion cloud, and Σ_i is the integrated conductivity for the background ionosphere. The initial conditions were of the form

$$\Sigma(x,y) / \Sigma_i = \left[1 + (M-1)\, e^{-(x^2 + y^2)/R^2}\right](1 + \epsilon(x,y)) \tag{11}$$

The five conductivity ratios were M = 2, 5, 15, 30, and 80. The Gaussian radius R was 1 km for all cases. The perturbation $\epsilon(x,y)$ was generated by assigning random phases to a Gaussian autocorrelation function, Fourier transforming from wavenumber space to physical space, and normalizing to a root-mean-square value of 0.03. The same sequence of random phases was used in all cases.

Equation (5) was integrated in time using a fully multidimensional leapfrog-trapezoidal flux-corrected transport (FCT) algorithm developed by Zalesak (1979). The algorithm is basically fourth order in space and second order in time, and uses a nonlinear flux-limiter to eliminate spurious oscillations due to numerical dispersion, while at the same time minimizing numerical diffusion. This is the same algorithm as that used in the previous work of

McDonald et al., (1978). Equation (7) was solved at each time level using a regridded Chebychev relaxation method (McDonald, 1977). The resulting code is vectorizable and executes at high efficiency on the Texas Instruments ASC.

The computational mesh consisted of 162 x 82 grid points in the x and y directions. The x direction is taken to be the direction of the neutral wind with respect to the ambient plasma. The mesh spacing was 30 m in both directions. The timestep was allowed to vary so as to attain the maximum value permitted by the Courant-Friedricks-Lewy (CFL) stability criterion. For the conductivity ratio set (2, 5, 15, 30, 80) the numbers of timesteps required to reach 240 sec were (800, 1943, 3725, 4896, 7520). The boundary conditions are periodic in y and Neumann in x ($\partial/\partial x = 0$). This gives a more realistic representation of inflow-outflow in the wind direction than doubly periodic or Dirichlet boundary conditions used in previous codes.

4. SUMMARY AND COMPARISON WITH DATA

Figures 7 and 8 summarize all five numerical simulations described above. Contour plots of Σ (x,y) are arranged with the conductivity ratio M increasing downward and time increasing to the right. This composite arrangement of contour plots makes clear the effect of total-to-background integrated conductivity ratio upon cloud evolution. At low and high cloud conductivities ($M \approx 1$ and $M \gg 1$) striation onset occurs late. At an intermediate M value, the onset time

attains a minimum. The M = 5 case develops most rapidly of the cases presented here, with onset at approximately 80 seconds, equivalent to eight linear growth times L/V. At low cloud conductivity, the interior of the cloud is shielded only weakly from the external electric field $\underline{E}_o$, so that all portions of the cloud tend to drift in a nearly solid body fashion at the ambient drift speed. At high cloud conductivity, the interior of the cloud is almost totally shilded from $\underline{E}_o$, resulting in a nearly solid body translation with the neutral wind. Irregularities do develop on the backside of the cloud in the M = 80 case, but they are convected rapidly around the cloud's perimeter and into the stable frontside. At the intermediate values of M, the interior of the cloud is only partially shielded from $\underline{E}_o$, resulting in appreciable velocity differences among different parts of the cloud. This accounts for the rapid development of striations at intermediate M values.

This is in qualitative agreement with a result of Linson (1975). Linson assumes an elliptically shaped cloud with constant interior and exterior plasma densities of different values (a waterbag model). In Figure 9 are plotted onset times (determined by visual inspection of contour plots) versus M. The filled dots are from Figures 7 and 8, while the unfilled dots are from earlier simulations not presented here. The solid curve is from Linson's (1975) waterbag model, for which

$$t_o = \frac{a}{V}\left[\frac{a}{b}\,\alpha + \left(1+2\,\frac{a}{b}\right) + \left(1+\frac{a}{b}\right)\alpha^{-1}\right], \qquad (12)$$

and

$$\alpha = M-1. \qquad (13)$$

In (12) a and b are the cloud's principal radii in the directions parallel and perpendicular to the neutral wind, respectively. For large M, a best fit to our results occurs for a = R and b = 2R. Exact agreement with this model is not to be expected since we have neither an elliptical cloud nor discontinuities between two constant densities. Linson's model best fits the highest conductivity ratios ($M \geq 5$) as one might expect. The severe steepening on the highest conductivity clouds results in a sharp drop in integrated conductivity from the cloud peak value to the background ionospheric value.

Irregularity power spectra descriptive of the late time results are shown in Figures 10 and 11. They are from the M = 30 case at 160 sec and 238 sec., respectively. In each case simulation results are plotted as dots. The solid lines are least-squares fits of the data to the spectral form of Rufenach (1974),

$$P(k) \propto (k^2 + k_o^2)^{N/2} \qquad (14)$$

The fit constants N and k_o are given in the upper right of each plot. The value of k_o is given in units of the fundamental wavenumber

$$k_1 = 2\pi/D \qquad (15)$$

In the y direction, D is the system size, 2.4 km. In the x direction, D is twice the system size, or 9.6 km because of the Neumann boundary condition in x. Each one dimensional spectrum is obtained by summing the two dimensional spectral power over the transverse wavenumber. Before complete bifurcation of the cloud (Figure 10) both x and y spectral indices N are between -2 and -3, in agreement with typical in situ observations (Kelley et al., 1979) made during the STRESS barium releases. After bifurcation of the cloud into several separate pieces (Figure 11), the x spectral index remains between -2 and -3, while the y index drops below -4.

The above spectral results are typical of all simulations presented here. Only the post-bifurcation y spectrum seems to be in disagreement with previously existing measurements. This is probably because in actual barium clouds complete bifurcation is seldom achieved. The evolution

of the Avefria Dos cloud before about 200 seconds (Figure 4) seems consistent with simulation results. Beyond 200 seconds, all simulation cases except M = 80 show complete bifurcation of the cloud into two or more parts. This is to be contrasted with the observed evolution shown in Figure 5 (314 sec). Fine structuring is evident, but complete bifurcation has not been achieved. The reason for this disagreement between simulation and experiment is not understood, but is a subject of continuing investigation.

Considering the dependence of onset time upon conductivity ratio evident in Figs. 7 and 8, what are the implications of the observed 135 sec onset time for Avefria Dos (Fig. 2)? If our estimates R = 1 km and V = 100 m/s are correct, then the observed onset time of 135 sec is in close agreement with the calculations for conductivity ratios M = 2 and 30. The estimated limits on the conductivity ratio given earlier then favor M = 30 as being the proper ratio. If however, the experimental data were R = 1.7 km as suggested by Linson (private communication, 1979), and V = 125 m/sec as suggested by Pongratz (private communication, 1978), the scaling law (9) implies that we should expect onset at 99 sec in the simulation. This would occur for M between 2 and 5 or between 15 and 30. The larger M values falls comfortably within the estimated range 3.5 - 32 given earlier. Thus, given moderate uncertainties in the values of the neutral wind speed and the cloud's effective Gaussian radius, the simulations suggest that the

conductivity ratio of the Avefria Dos was between 15 and 30.

Despite some unresolved difference at late times, the numerical simulation results presented here definitely show that physically small (Gaussian radius $\approx$ 1 km) barium clouds will attain well developed structure much more rapidly than large (Gaussian radius 5-10km) barium clouds, all other parameters being similar. Indeed, these times can be an order of magnitude different.

Acknowledgement

This work was supported by the Defense Nuclear Agency. Also, the authors would like to thank M. Pongratz of LASL for providing Figures 1-5 and allowing us to use them in this paper.

REFERENCES

Banks, P. M., and G. Kockarts, Aeronomy (Part A), Academic Press, New York, 1973.

Davis, T. N., G. J. Romick, E. M. Westcott, R. A. Jeffires, D. M. Kerr, and H. M. Peek, Observations of the development of striations in large barium clouds, Planet. Space Sci., 22, 67, 1974.

Doles, J. H., III, N. J. Zabusky, and F. W. Perkins, Deformation and striation of plasma clouds in the ionosphere 3. Numerical simulations of a multilevel model with recombination chemistry, J. Geophys. Res., 81, 5987, 1976.

Francis, S. H., and F. W. Perkins, Determination of striation scale sizes for plasma clouds in the ionosphere, J. Geophys. Res., 80, 3111, 1975.

Kelley, M. C., K. D. Baker, and J. C. Ulwick, Late time barium clouds and their possible relationship to equatorial Spread F, J. Geophys. Res., 84, 1898, 1979.

Linson, L. M., Slab release and onset time of striations; in Multiple barium release studies, KMR Ionospheric Monitoring Program, Spring, 1975, HAPREX Final Report V.3, Stanford Research Institute, Menlo Park, Calif., October, 1975.

McDonald, B. E., Explicit Chebychev-iterative solution of nonself-adjoint elliptic equations on a vector computer, NRL Memo Report 3541, Naval Res. Lab., Washington, D. C., June, 1977.

McDonald, B. E., S. L. Ossakow, S. T. Zalesak, and N. J. Zabusky, Determination of minimum scale sizes in plasma cloud striations, Proceedings of 1978 Symposium on the Effect of the Ionosphere on Space and Terrestrial Systems, ed J. M. Goodman U.S. Government Printing Office, Washington, D. C., 1978.

Pongratz, M. B., G. M. Smith, R. C. Carlos, H. G. Horak, D. J. Simmons, and C. F. Lebeda, High spatial resolution field-aligned observations of gradient-drift formation in barium clouds, Eos Trans. AGU, 59, 1161, 1978.

Rufenach, C. L., Wavelength dependence of radio scintillation: Ionosphere and interplanetary irregularities, J. Geophys. Res., 79, 1562, 1974.

Scannapieco, A. J., S. L. Ossakow, D. L. Book, B. E. McDonald, and S. R. Goldman, Conductivity ratio effects on the drift and deformation of F-region barium clouds coupled to the E region ionosphere, J. Geophys. Res. 79, 2913, 1974.

Scannapieco, A. J., S. L. Ossakow, S. R. Goldman, and J. M. Pierre, "Plasma cloud late time striation spectra," J. Geophys. Res., 81, 6037, 1976.

Volk, H. J. and G. Haerendel, Striations in ionospheric ion clouds, J. Geophys. Res., 76, 4541, 1971.

Zalesak, S. T., Fully multidimensional flux-corrected transport algorithms for fluids, J. Comp. Phys, 31, 335, 1979.

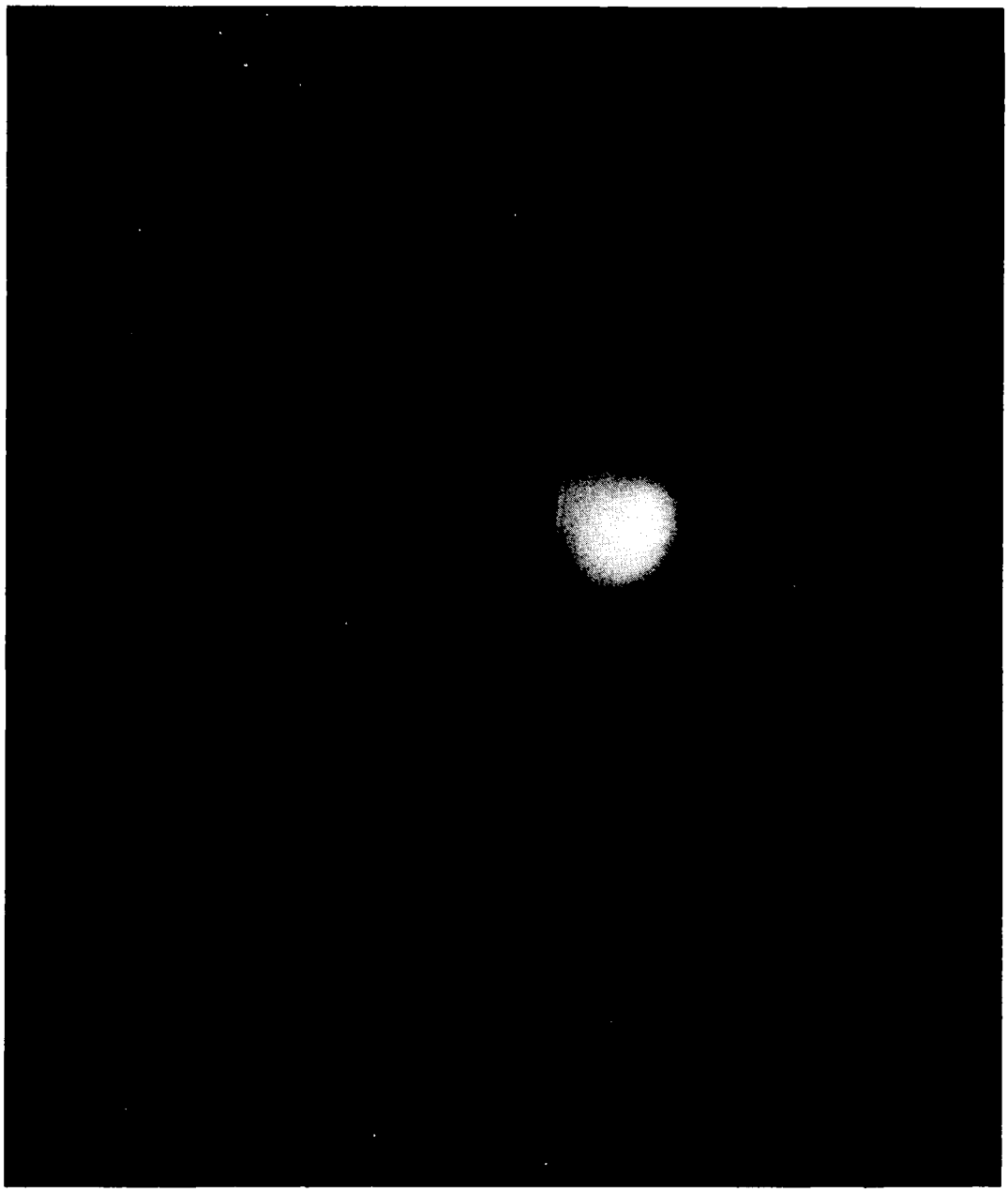

Fig. 1 - Avefria Uno at 22 seconds photographed at a station almost directly below the detonation point. The magnetic dip angle is approximately 65°. Small scale structures parallel to the magnetic field are believed to be the result of kinetic instabilities.

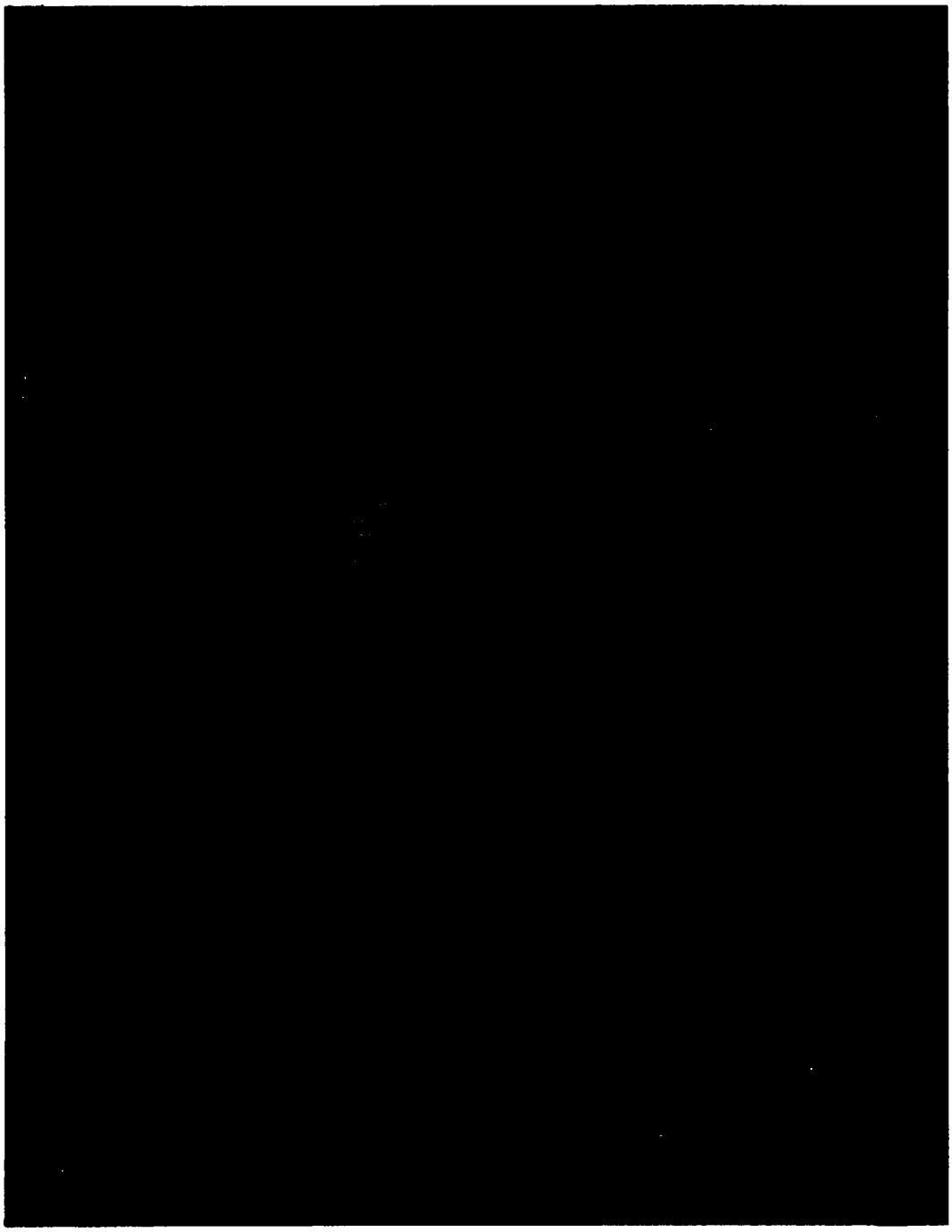

Fig. 2 - Avefria Dos at 135 seconds photographed at a station nominally on the same geomagnetic field line as the detonation point. Thus the plane of the photograph is transverse to $\underline{B}$. At 135 seconds, gradient drift striations are just beginning to emerge.

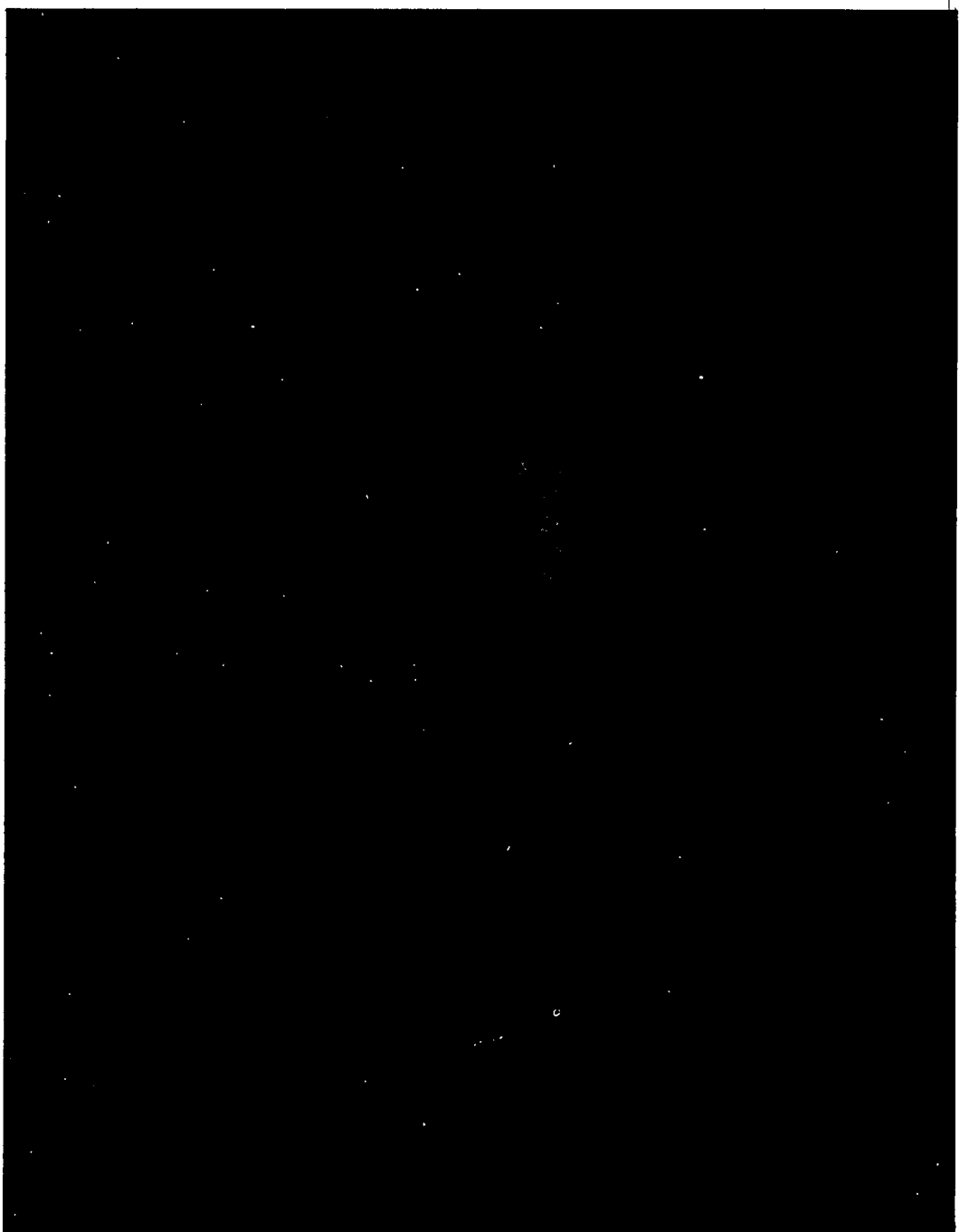

Fig. 3 - Same as Figure 2 at 151 seconds

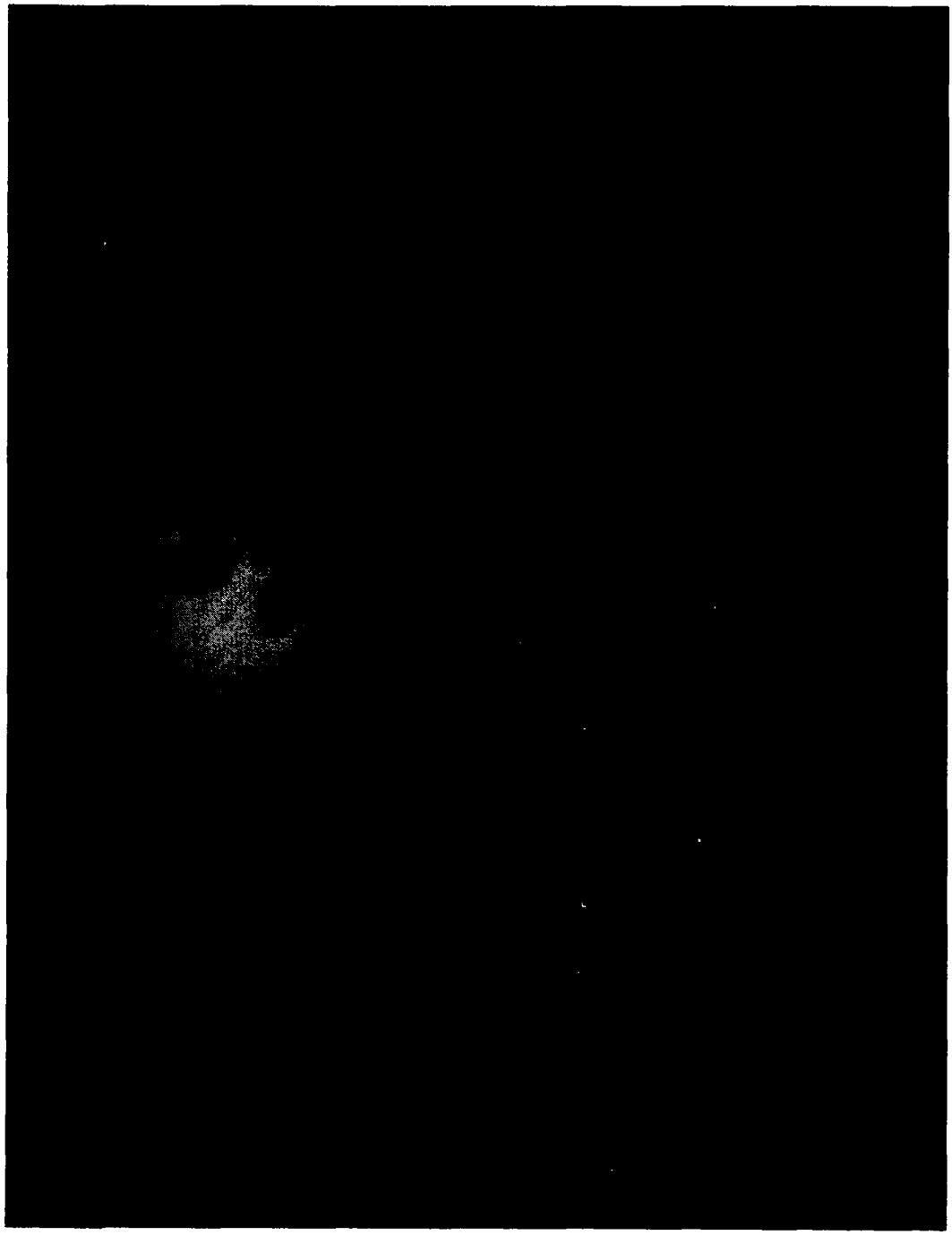

Fig. 4 - Same as Figure 2 at 211 seconds

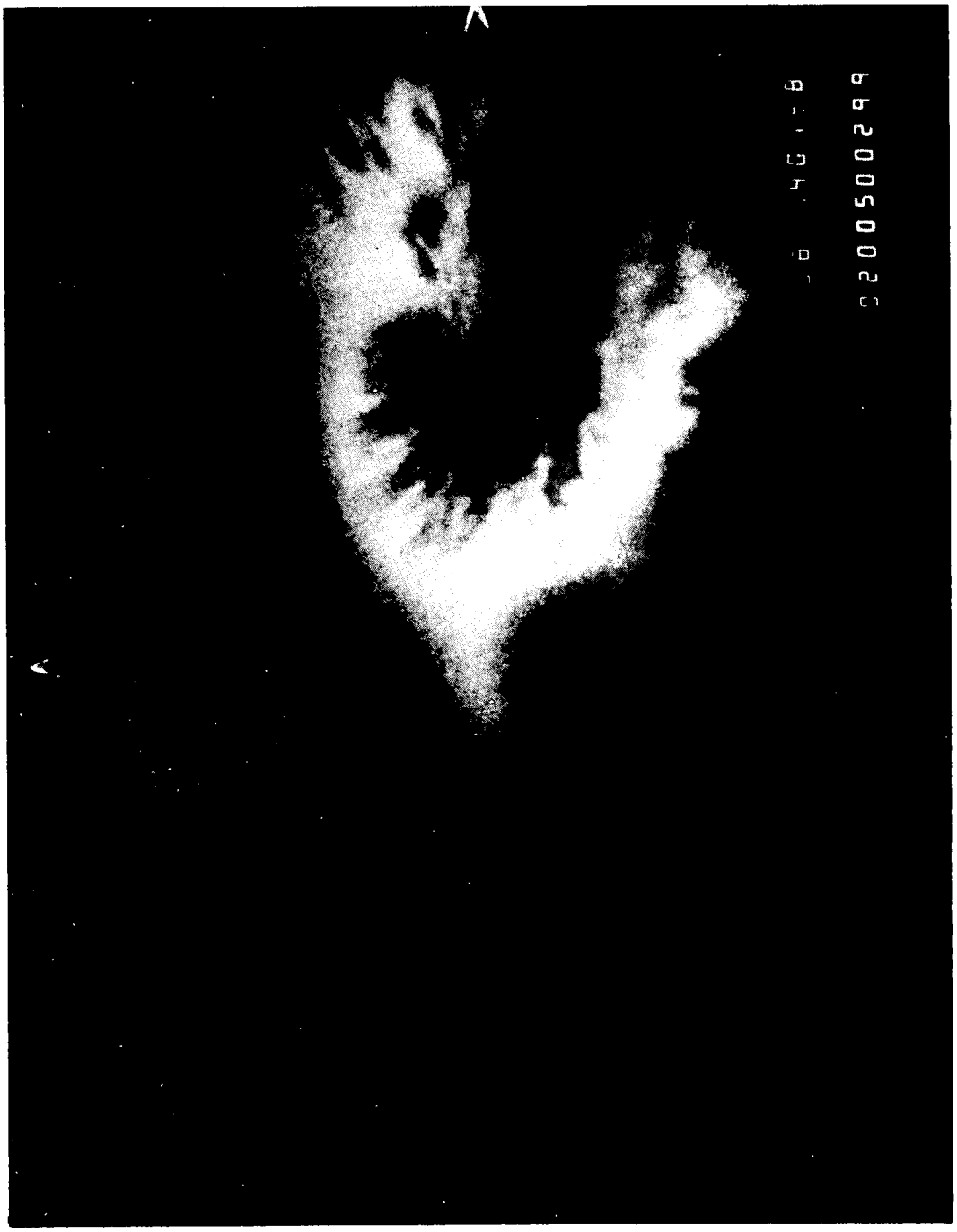

Fig. 5 - Same as Figure 2 at 314 seconds

Fig. 6 - Event Spruce (February, 1971) at 24 minutes. The age of Spruce at this point in terms of linear growth times is comparable to that of Avefria Dos in Figure 5. Notice, however, the distinct contrast in the shapes of the striations.

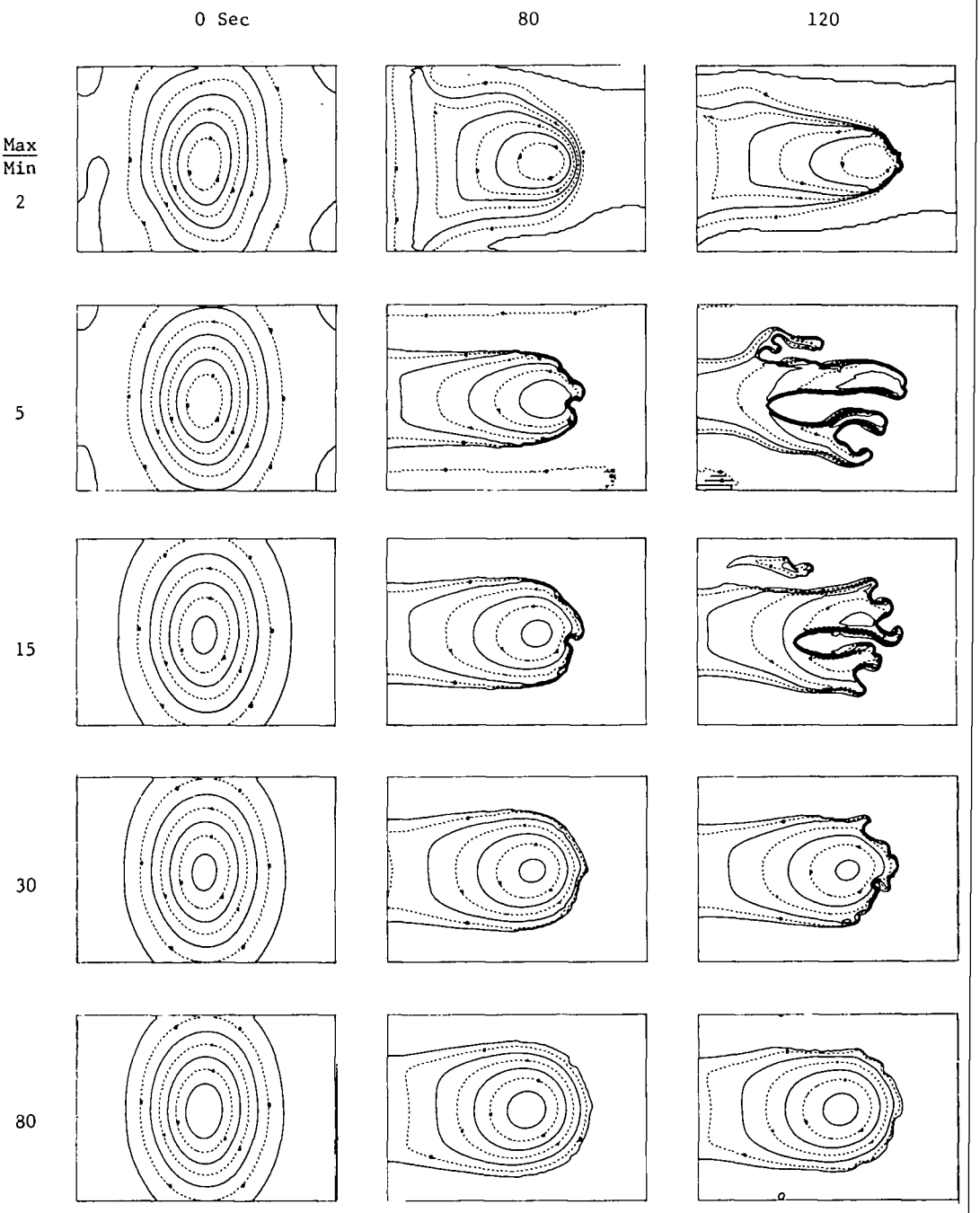

Fig. 7 - Simulated cloud evolution for various values of peak-to-background integrated Pedersen conductivity ratios. Time increases to the right and conductivity ratio increases downward.

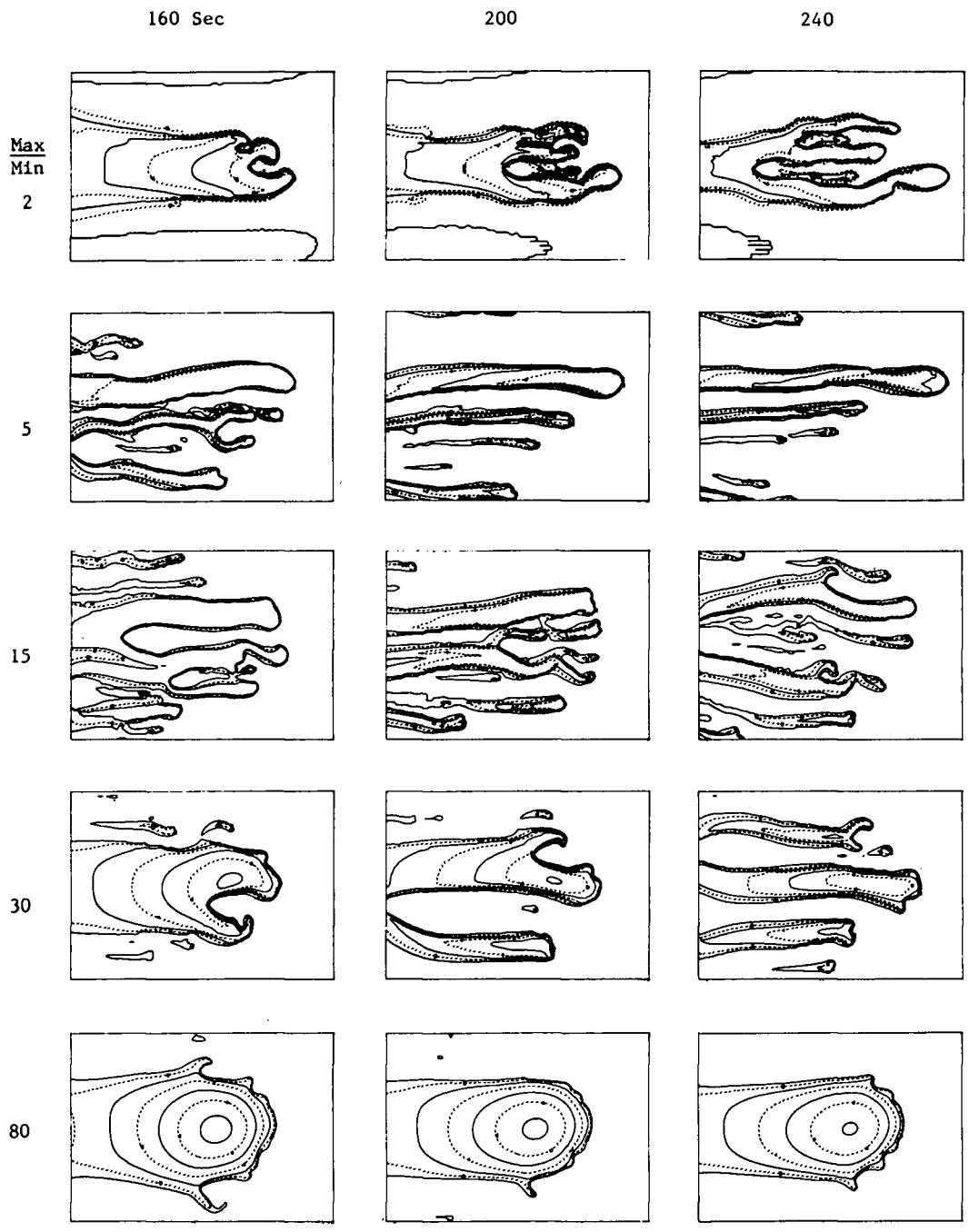

Fig. 8 - Simulated cloud evolution for various values of peak-to-background integrated Pedersen conductivity ratios. Time increases to the right and conductivity ratio increases downward.

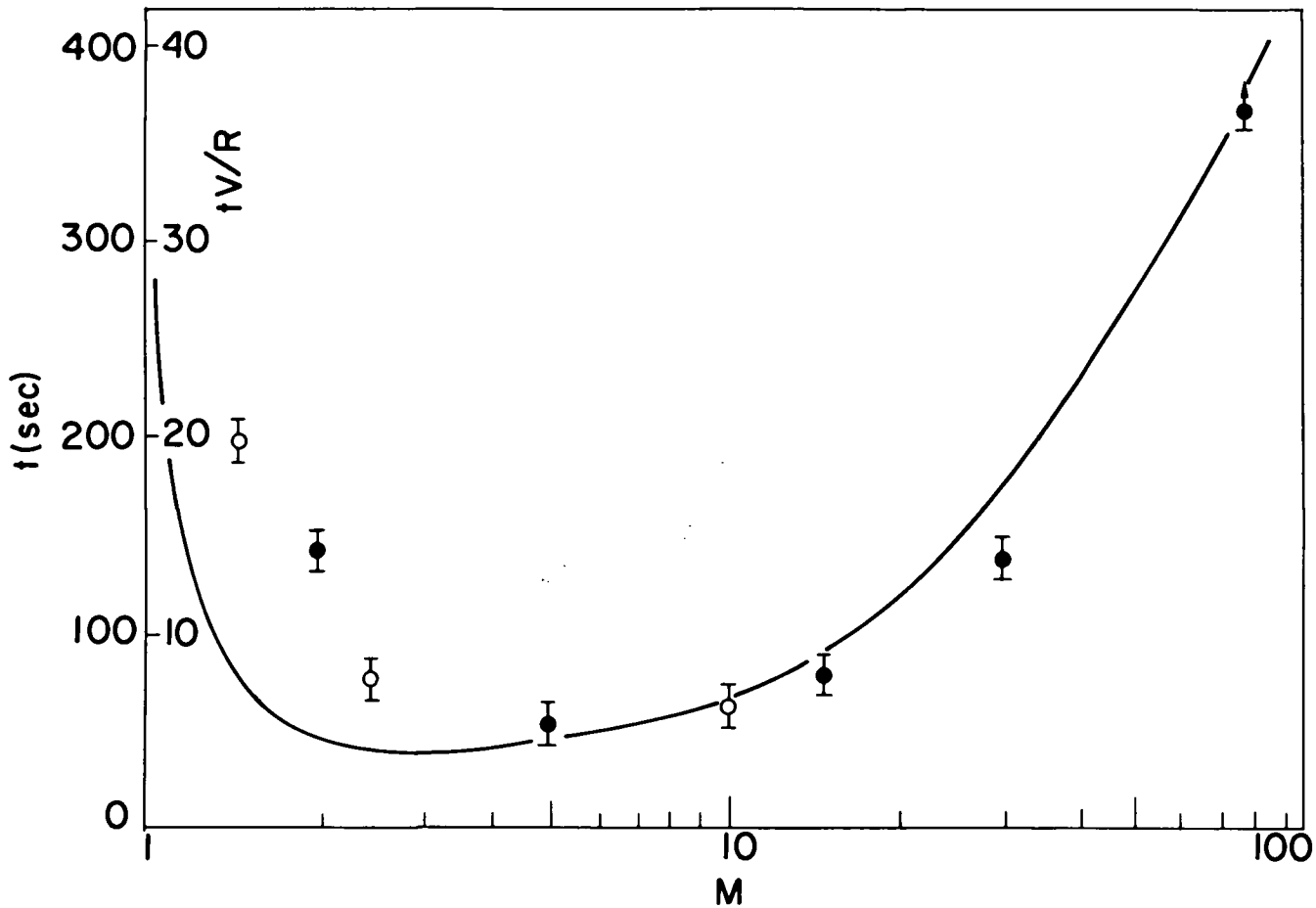

Fig. 9 - Onset times (expressed in seconds and linear growth times) for simulated clouds as a function of conductivity ratio M. The solid curve is from a waterbag model (see eq. (12)). Solid dots are obtained from visual inspection of simulation results summarized in Figures 7 and 8. Unfilled dots are from previous simulations not presented here. Error bars are set somewhat arbitrarily at $\pm$ 1 linear growth time. The M = 80 case has no upper error bar because bifurcation was not achieved.

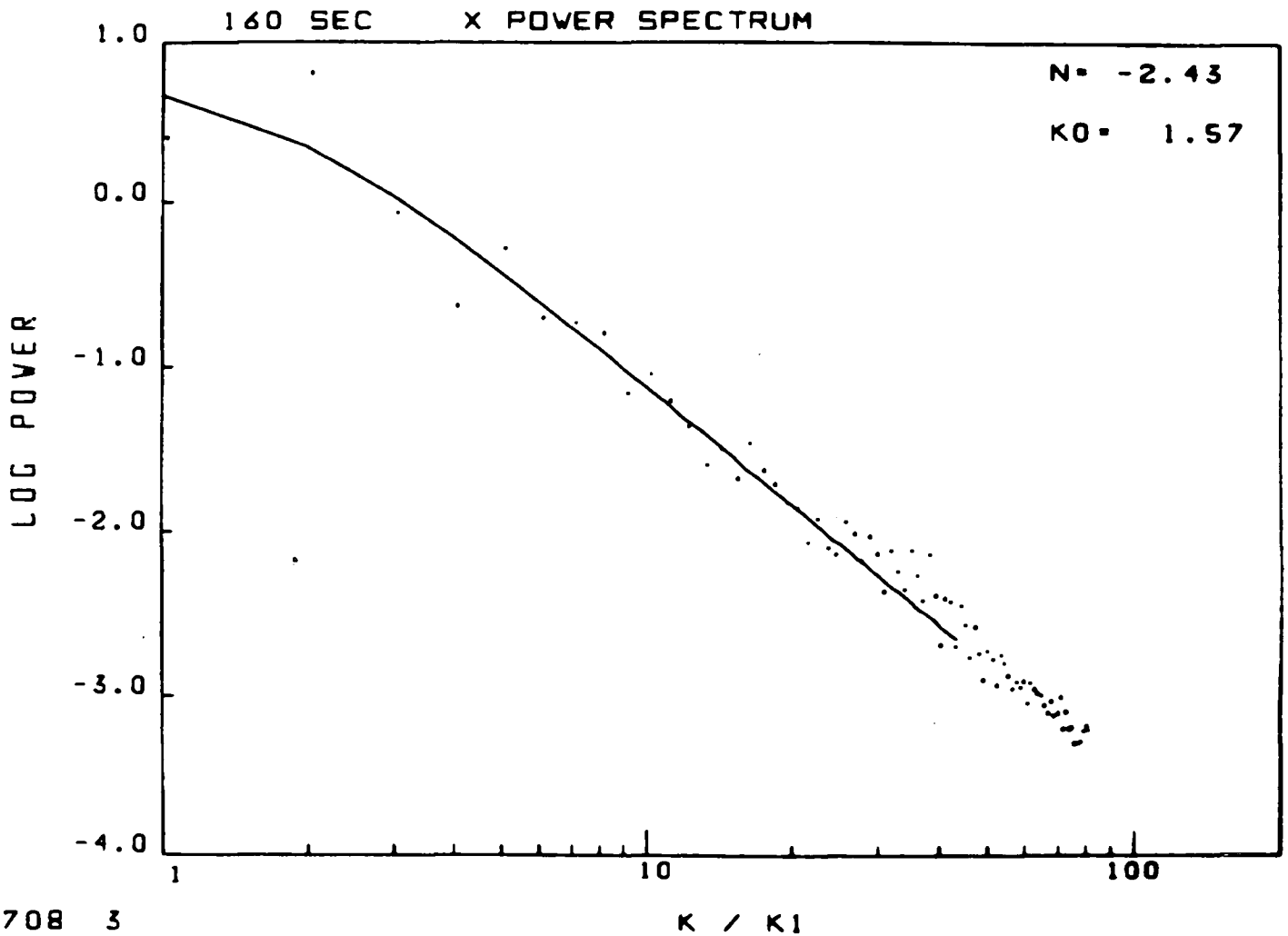

Fig. 10a - Striation power spectra (arbitrary units) for the M = 30 case at 160 seconds. N and k_o describe the Rufenach spectrum (solid line; see (14)) which best fits the simulation data points.

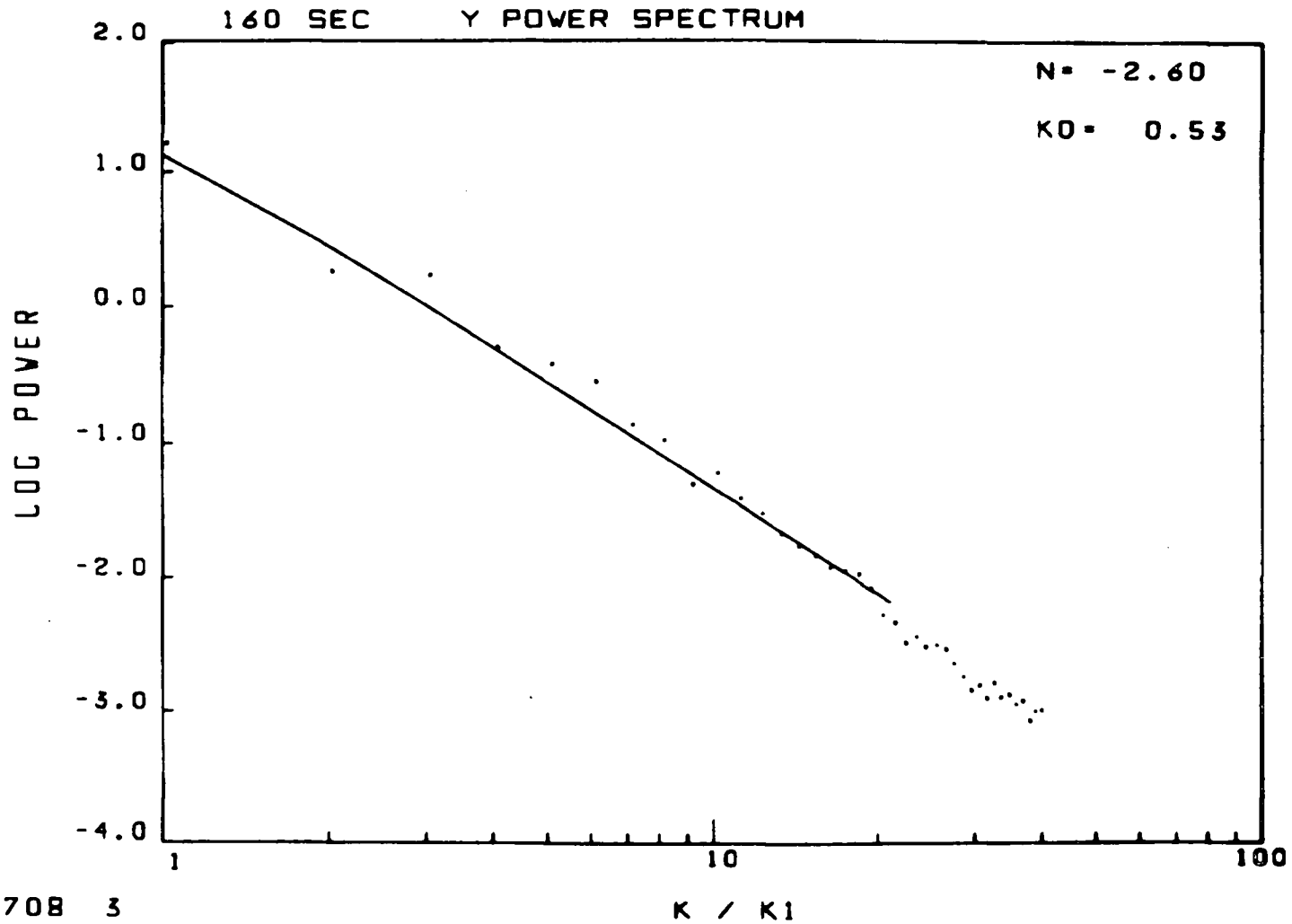

Fig. 10b - Striation power spectra (arbitrary units) for the M = 30 case at 160 seconds. N and k_o describe the Rufenach spectrum (solid line; see (14)) which best fits the simulation data points.

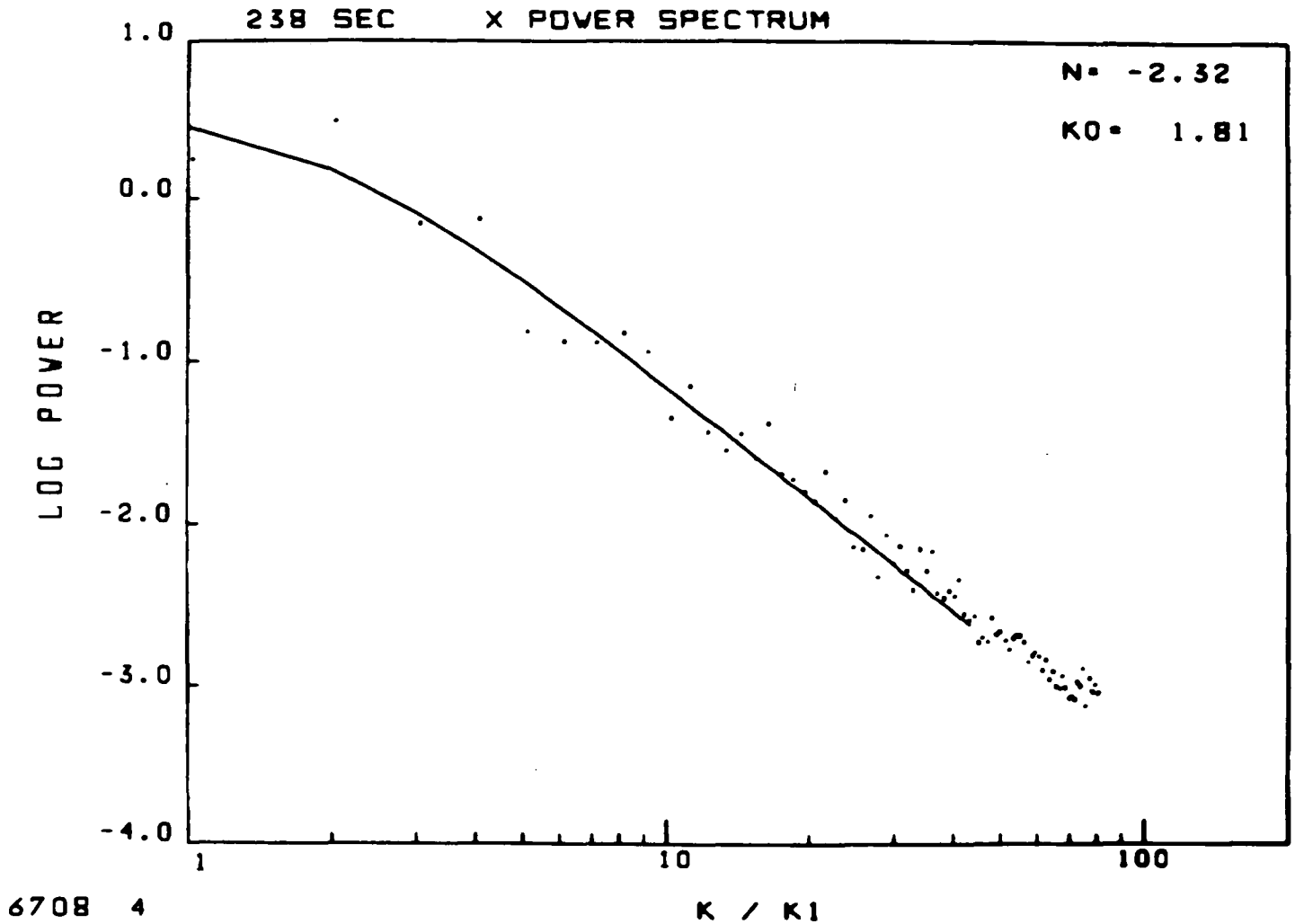

Fig. 11a - Same as Figure 10 for 238 seconds. The 2 second departure from the nominal 240 second display time of Figure 8 is a result of variable timestepping.

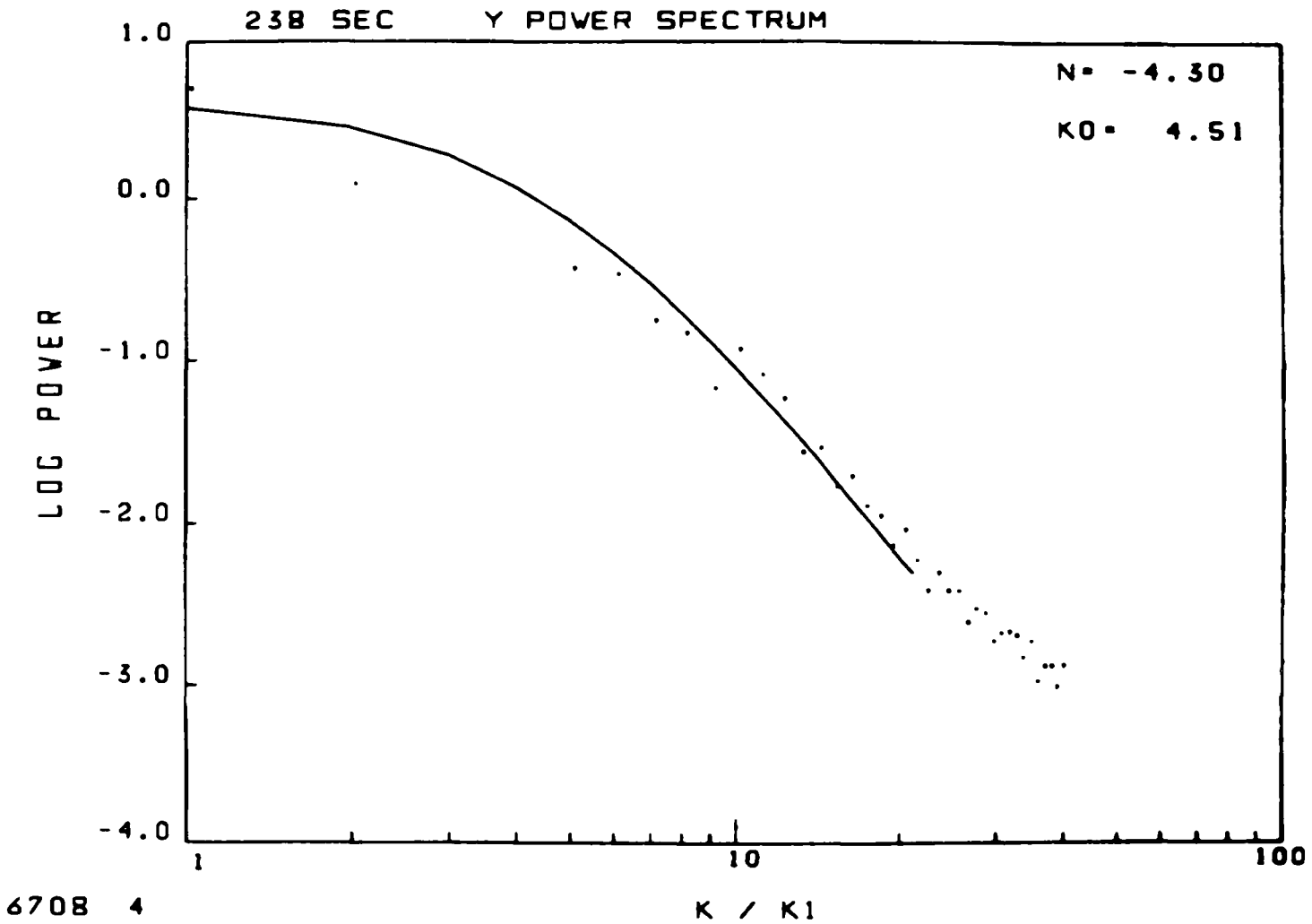

Fig. 11b - Same as Figure 10 for 238 seconds. The 2 second departure from the nominal 240 second display time of Figure 8 is a result of variable timestepping.

DISTRIBUTION LIST

DEPARTMENT OF DEFENSE

ASSISTANT SECRETARY OF DEFENSE
COMM, CMD, CONT & INTELL
WASHINGTON, D.C. 20301
01CY ATTN J. BABCOCK
01CY ATTN M. EPSTEIN

ASSISTANT TO THE SECRETARY OF DEFENSE
ATOMIC ENERGY
WASHINGTON, D.C. 20301
01CY ATTN EXECUTIVE ASSISTANT

DIRECTOR
COMMAND CONTROL TECHNICAL CENTER
PENTAGON RM BE 685
WASHINGTON, D.C. 20301
01CY ATTN C-650
01CY ATTN C-312 R. MASON

DIRECTOR
DEFENSE ADVANCED RSCH PROJ AGENCY
ARCHITECT BUILDING
1400 WILSON BLVD.
ARLINGTON, VA. 22209
01CY ATTN NUCLEAR MONITORING RESEARCH
01CY ATTN STRATEGIC TECH OFFICE

DEFENSE COMMUNICATION ENGINEER CENTER
1860 WIEHLE AVENUE
RESTON, VA. 22090
01CY ATTN CODE R820
01CY ATTN CODE R410 JAMES W. MCLEAN
01CY ATTN CODE R720 J. WORTHINGTON

DIRECTOR
DEFENSE COMMUNICATIONS AGENCY
WASHINGTON, D.C. 20305
(ADR CNWDI: ATTN CODE 240 FOR)
01CY ATTN CODE 480
01CY ATTN CODE 810 R. W. ROSTRON
01CY ATTN CODE 101B
01CY ATTN CODE 103 M. RAFFENSPERGER

DEFENSE DOCUMENTATION CENTER
CAMERON STATION
ALEXANDRIA, VA. 22314
(12 COPIES IF OPEN PUBLICATION, OTHERWISE 2 COPIES)
12CY ATTN TC

DIRECTOR
DEFENSE INTELLIGENCE AGENCY
WASHINGTON, D.C. 20301
01CY ATTN DT-1B
01CY ATTN DB-4C E. O'FARRELL
01CY ATTN DIAAP A. WISE
01CY ATTN DIAST-5
01CY ATTN DT-1BZ R. MORTON
01CY ATTN HQ-TR J. STEWART
01CY ATTN W. WITTIG DC-7D

DIRECTOR
DEFENSE NUCLEAR AGENCY
WASHINGTON, D.C. 20305
01CY ATTN STVL
04CY ATTN TITL
01CY ATTN DDST
03CY ATTN RAAE

COMMANDER
FIELD COMMAND
DEFENSE NUCLEAR AGENCY
KIRTLAND AFB, NM 87115
01CY ATTN FCPR

DIRECTOR
INTERSERVICE NUCLEAR WEAPONS SCHOOL
KIRTLAND AFB, NM 87115
01CY ATTN DOCUMENT CONTROL

JOINT CHIEFS OF STAFF
WASHINGTON, D.C. 20301
01CY ATTN J-3 WWMCCS EVALUATION OFFICE

DIRECTOR
JOINT STRAT TGT PLANNING STAFF
OFFUTT AFB
OMAHA, NB 68113
01CY ATTN JLTW-2
01CY ATTN JPST G. GOETZ

CHIEF
LIVERMORE DIVISION FLD COMMAND DNA
DEPARTMENT OF DEFENSE
LAWRENCE LIVERMORE LABORATORY
P. O. BOX 808
LIVERMORE, CA 94550
01CY ATTN FCPRL

DIRECTOR
NATIONAL SECURITY AGENCY
DEPARTMENT OF DEFENSE
FT. GEORGE G. MEADE, MD 20755
01CY ATTN JOHN SKILLMAN R52
01CY ATTN FRANK LEONARD
01CY ATTN W14 PAT CLARK
01CY ATTN OLIVER H. BARTLETT W32
01CY ATTN R5

COMMANDANT
NATO SCHOOL (SHAPE)
APO NEW YORK 09172
01CY ATTN U.S. DOCUMENTS OFFICER

UNDER SECY OF DEF FOR RSCH & ENGRG
DEPARTMENT OF DEFENSE
WASHINGTON, D.C. 20301
01CY ATTN STRATEGIC & SPACE SYSTEMS (OS)

WWMCCS SYSTEM ENGINEERING ORG
WASHINGTON, D.C. 20305
01CY ATTN R. CRAWFORD

COMMANDER/DIRECTOR
ATMOSPHERIC SCIENCES LABORATORY
U.S. ARMY ELECTRONICS COMMAND
WHITE SANDS MISSILE RANGE, NM 88002
01CY ATTN DELAS-EO F. NILES

DIRECTOR
BMD ADVANCED TECH CTR
HUNTSVILLE OFFICE
P. O. BOX 1500
HUNTSVILLE, AL 35807
01CY ATTN ATC-T MELVIN T. CAPPS
01CY ATTN ATC-O W. DAVIES
01CY ATTN ATC-R DON RUSS

PROGRAM MANAGER
BMD PROGRAM OFFICE
5001 EISENHOWER AVENUE
ALEXANDRIA, VA 22333
01CY ATTN DACS-BMT J. SHEA

CHIEF C-E SERVICES DIVISION
U.S. ARMY COMMUNICATIONS CMD
PENTAGON RM 1B269
WASHINGTON, D.C. 20310
01CY ATTN C-E-SERVICES DIVISION

COMMANDER
FRADCOM TECHNICAL SUPPORT ACTIVITY
DEPARTMENT OF THE ARMY
FORT MONMOUTH, N.J. 07703
01CY ATTN DRSEL-NL-RD H. BENNET
01CY ATTN DRSEL-PL-ENV H. BOMKE
01CY ATTN J. E. QUIGLEY

COMMANDER
HARRY DIAMOND LABORATORIES
DEPARTMENT OF THE ARMY
2800 POWDER MILL ROAD
ADELPHI, MD 20783
(CNWDI-INNER ENVELDPE: ATTN: DELHD-RBH)
01CY ATTN DELHD-TI M. WEINER
01CY ATTN DELHD-RB R. WILLIAMS
01CY ATTN DELHD-NP F. WIMENITZ
01CY ATTN DELHD-NP C. MDAZED

COMMANDER
U.S. ARMY COMM-ELEC ENGRG INSTAL AGY
FT. HUACHUCA, AZ 85613
01CY ATTN CCC-EMED GEORGE LANE

COMMANDER
U.S. ARMY FDREIGN SCIENCE & TECH CTR
220 7TH STREET, NE
CHARLOTTESVILLE, VA 22901
01CY ATTN DRXST-SD
01CY ATTN R. JONES

COMMANDER
U.S. ARMY MATERIEL DEV & READINESS CMD
5001 EISENHOWER AVENUE
ALEXANDRIA, VA 22333
01CY ATTN DRCLDC J. A. BENDER

CDMMANDER
U.S. ARMY NUCLEAR AND CHEMICAL AGENCY
7500 BACKLICK ROAD
BLDG 2073
SPRINGFIELD, VA 22150
01CY ATTN LIBRARY

DIRECTOR
U.S. ARMY BALLISTIC RESEARCH LABS
ABERDEEN PRDVING GROUND, MD 21005
01CY ATTN TECH LIB EDWARD BAICY

COMMANDER
U.S. ARMY SATCOM AGENCY
FT. MONMOUTH, NJ 07703
01CY ATTN DOCUMENT CONTROL

COMMANDER
U.S. ARMY MISSILE INTELLIGENCE AGENCY
REDSTONE ARSENAL, AL 35809
01CY ATTN JIM GAMBLE

DIRECTOR
U.S. ARMY TRADOC SYSTEMS ANALYSIS ACTIVITY
WHITE SANDS MISSILE RANGE, NM 88002
01CY ATTN ATAA-SA
01CY ATTN TCC/F. PAYAN JR.
01CY ATTN ATAA-TAC LTC J. HESSE

COMMANDER
NAVAL ELECTRONIC SYSTEMS COMMAND
WASHINGTON, D.C. 20360
01CY ATTN NAVALEX 034 T. HUGHES
01CY ATTN PME 117
01CY ATTN PME 117-T
01CY ATTN CDDE 5011

COMMANDING DFFICER
NAVAL INTELLIGENCE SUPPORT CTR
4301 SUITLAND ROAD, BLDG. 5
WASHINGTON, D.C. 20390
01CY ATTN MR. DUBBIN STIC 12
01CY ATTN NISC-50
01CY ATTN CODE 5404 J. GALET

COMMANDER
NAVAL SURFACE WEAPONS CENTER
DAHLGREN LABORATORY
DAHLGREN, VA 22448
01CY ATTN CDDE DF-14 R. BUTLER

COMMANDING OFFICER
NAVY SPACE SYSTEMS ACTIVITY
P.O. BOX 92960
WDRLDWAY PDSTAL CENTER
LDS ANGELES, CA. 90009
01CY ATTN CDDE 52

DFFICE OF NAVAL RESEARCH
ARLINGTON, VA 22217
01CY ATTN CODE 465
01CY ATTN CODE 461
01CY ATTN CDDE 402
01CY ATTN CODE 420
01CY ATTN CODE 421

COMMANDER
AEROSPACE DEFENSE COMMAND/DC
DEPARTMENT OF THE AIR FDRCE
ENT AFB, CD 80912
01CY ATTN DC MR. LONG

COMMANDER
AERDSPACE DEFENSE COMMAND/XPD
DEPARTMENT OF THE AIR FDRCE
ENT AFB, CO 80912
01CY ATTN XPDQQ
01CY ATTN XP

AIR FDRCE GEOPHYSICS LABORATDRY
HANSCOM AFB, MA 01731
01CY ATTN DPR HAROLD GARDNER
01CY ATTN DPR-1 JAMES C. ULWICK
01CY ATTN LKB KENNETH S. W. CHAMPION
01CY ATTN DPR ALVA T. STAIR
01CY ATTN PHP JULES AARONS
01CY ATTN PHD JURGEN BUCHAU
01CY ATTN PHD JOHN P. MULLEN

AF WEAPONS LABORATORY
KIRTLAND AFB, NM 87117
01CY ATTN SUL
01CY ATTN CA ARTHUR H. GUENTHER
01CY ATTN DYC CAPT J. BARRY
01CY ATTN DYC JOHN M. KAMM
01CY ATTN DYT CAPT MARK A. FRY
01CY ATTN DES MAJ GARY GANONG
01CY ATTN DYC J. JANNI

AFTAC
PATRICK AFB, FL 32925
01CY ATTN TF/MAJ WILEY
01CY ATTN TN

AIR FORCE AVIONICS LABORATDRY
WRIGHT-PATTERSON AFB, OH 45433
01CY ATTN AAD WADE HUNT
01CY ATTN AAD ALLEN JOHNSON

DEPUTY CHIEF OF STAFF
RESEARCH, DEVELDPMENT, & ACQ
DEPARTMENT OF THE AIR FDRCE
WASHINGTON, D.C. 20330
01CY ATTN AFRDQ

HEADQUARTERS
ELECTRONIC SYSTEMS DIVISION/XR
DEPARTMENT OF THE AIR FDRCE
HANSCOM AFB, MA 01731
01CY ATTN XR J. DEAS

HEADQUARTERS
ELECTRONIC SYSTEMS DIVISION/YSEA
DEPARTMENT OF THE AIR FORCE
HANSCOM AFB, MA 01731
01CY ATTN YSEA

COMMANDER
NAVAL OCEAN SYSTEMS CENTER
SAN DIEGO, CA 92152
03CY ATTN CODE 532 W. MOLER
01CY ATTN CODE 0230 C. BAGGETT
01CY ATTN CODE 81 R. EASTMAN

DIRECTOR
NAVAL RESEARCH LABORATORY
WASHINGTON, D.C. 20375
01CY ATTN CODE 6700 TIMOTHY P. COFFEY
(25 CYS IF UNCLASS, 1 CY IF CLASS)
01CY ATTN CODE 6701 JACK O. BROWN
01CY ATTN CODE 6780 BRANCH HEAD (150 CYS IF UNCLASS, 1 CY IF CLASS)
01CY ATTN CODE 7500 HQ COMM DIR BRUCE WALD
01CY ATTN CODE 7550 J. DAVIS
01CY ATTN CODE 7580
01CY ATTN CODE 7551
01CY ATTN CODE 7555
01CY ATTN CODE 6730 E. MCLEAN
01CY ATTN CODE 7127 C. JOHNSON

COMMANDER
NAVAL SEA SYSTEMS COMMAND
WASHINGTON, D.C. 20362
01CY ATTN CAPT R. PITKIN

COMMANDER
NAVAL SPACE SURVEILLANCE SYSTEM
DAHLGREN, VA 22448
01CY ATTN CAPT J. H. BURTON

OFFICER-IN-CHARGE
NAVAL SURFACE WEAPONS CENTER
WHITE OAK, SILVER SPRING, MD 20910
01CY ATTN CODE F31

DIRECTOR
STRATEGIC SYSTEMS PROJECT OFFICE
DEPARTMENT OF THE NAVY
WASHINGTON, D.C. 20376
01CY ATTN NSP-2141
01CY ATTN NSSP-2722 FRED WIMBERLY

NAVAL SPACE SYSTEM ACTIVITY
P. O. BOX 92960
WORLDWAY POSTAL CENTER
LOS ANGELES, CALIF. 90009
01CY ATTN A. B. HAZZARD

HEADQUARTERS
ELECTRONIC SYSTEMS DIVISION/DC
DEPARTMENT OF THE AIR FORCE
HANSCOM AFB, MA 01731
01CY ATTN DCKC MAJ J. C. CLARK

HEADQUARTERS
ELECTRONIC SYSTEMS DIVISION, AFSC
HANSCOM AFB, MA 01731
01CY ATTN XRW
01CY ATTN JAMES WHELAN

COMMANDER
FOREIGN TECHNOLOGY DIVISION, AFSC
WRIGHT-PATTERSON AFB, OH 45433
01CY ATTN NICD LIBRARY
01CY ATTN ETDP B. BALLARD

COMMANDER
ROME AIR DEVELOPMENT CENTER, AFSC
GRIFFISS AFB, NY 13441
01CY ATTN DOC LIBRARY/TSLD
01CY ATTN OCSE V. COYNE

SAMSO/SZ
POST OFFICE BOX 92960
WORLDWAY POSTAL CENTER
LOS ANGELES, CA 90009
(SPACE DEFENSE SYSTEMS)
01CY ATTN SZJ

STRATEGIC AIR COMMAND/XPFS
OFFUTT AFB, NB 68113
01CY ATTN XPFS MAJ B. STEPHAN
01CY ATTN ADWATE MAJ BRUCE BAUER
01CY ATTN NRT
01CY ATTN DOK CHIEF SCIENTIST

SAMSO/YA
P. O. BOX 92960
WORLDWAY POSTAL CENTER
LOS ANGELES, CA 90009
01CY ATTN YAT CAPT L. BLACKWELDER

SAMSO/SK
P. O. BOX 92960
WORLDWAY POSTAL CENTER
LOS ANGELES, CA 90009
01CY ATTN SKA (SPACE COMM SYSTEMS) M. CLAVIN

SAMSO/MN
NORTON AFB, CA 92409
(MINUTEMAN)
01CY ATTN MNNL LTC KENNEDY

COMMANDER
ROME AIR DEVELOPMENT CENTER, AFSC
HANSCOM AFB, MA 01731
01CY ATTN EEP A. LORENTZEN

DEPARTMENT OF ENERGY

DEPARTMENT OF ENERGY
ALBUQUERQUE OPERATIONS OFFICE
P. O. BOX 5400
ALBUQUERQUE, NM 87115
01CY ATTN DOC CON FOR D. SHERWOOD

DEPARTMENT OF ENERGY
LIBRARY ROOM G-042
WASHINGTON, D.C. 20545
01CY ATTN DOC CON FOR A. LABOWITZ

EG&G, INC.
LOS ALAMOS DIVISION
P. O. BOX 809
LOS ALAMOS, NM 85544
01CY ATTN DOC CON FOR J. BREEDLOVE

UNIVERSITY OF CALIFORNIA
LAWRENCE LIVERMORE LABORATORY
P. O. BOX 808
LIVERMORE, CA 94550
01CY ATTN DOC CON FOR TECH INFO DEPT
01CY ATTN DOC CON FOR L-389 R. OTT
01CY ATTN DOC CON FOR L-31 R. HAGER
01CY ATTN DOC CON FOR L-46 F. SEWARD

LOS ALAMOS SCIENTIFIC LABORATORY
P. O. BOX 1663
LOS ALAMOS, NM 87545
01CY ATTN DOC CON FOR J. WOLCOTT
01CY ATTN DOC CON FOR R. F. TASCHEK
01CY ATTN DOC CON FOR E. JONES
01CY ATTN DOC CON FOR J. MALIK
01CY ATTN DOC CON FOR R. JEFFRIES
01CY ATTN DOC CON FOR J. ZINN
01CY ATTN DOC CON FOR P. KEATON
01CY ATTN DOC CON FOR D. WESTERVELT

SANDIA LABORATORIES
P. O. BOX 5800
ALBUQUERQUE, NM 87115
01CY ATTN DOC CON FOR J. MARTIN
01CY ATTN DOC CON FOR W. BROWN
01CY ATTN DOC CON FOR A. THORNBROUGH
01CY ATTN DOC CON FOR T. WRIGHT
01CY ATTN DOC CON FOR D. DAHLGREN
01CY ATTN DOC CON FOR 3141
01CY ATTN DOC CON FOR SPACE PROJECT DIV

SANDIA LABORATORIES
LIVERMORE LABORATORY
P. O. BOX 969
LIVERMORE, CA 94550
01CY ATTN OOC CON FOR B. MURPHEY
01CY ATTN OOC CON FOR T. COOK

OFFICE OF MILITARY APPLICATION
OEPARTMENT OF ENERGY
WASHINGTON, D.C. 20545
01CY ATTN OOC CON FOR O. GALE

OTHER GOVERNMENT

CENTRAL INTELLIGENCE AGENCY
ATTN RO/SI, RM 5G48, HQ BLDG
WASHINGTON, D.C. 20505
01CY ATTN OSI/PSIO RM 5F 19

DEPARTMENT OF COMMERCE
NATIONAL BUREAU OF STANDAROS
WASHINGTON, O.C. 20234
(ALL CORRES: ATTN SEC OFFICER FOR)
01CY ATTN R. MOORE

OEPARTMENT OF TRANSPORTATION
OFFICE OF THE SECRETARY
TAD-44.1, ROOM 10402-B
400 7TH STREET, S.W.
WASHINGTON, O.C. 20590
01CY ATTN R. LEWIS
01CY ATTN R. OOHERTY

INSTITUTE FOR TELECOM SCIENCES
NATIONAL TELECOMMUNICATIONS & INFO ADMIN
BOULDER, CO 80303
01CY ATTN A. JEAN (UNCLASS ONLY)
01CY ATTN W. UTLAUT
01CY ATTN O. CROMBIE
01CY ATTN L. BERRY

NATIONAL OCEANIC & ATMOSPHERIC ADMIN
ENVIRONMENTAL RESEARCH LABORATORIES
OEPARTMENT OF COMMERCE
BOULDER, CO 80302
01CY ATTN R. GRUBB
01CY ATTN AERONOMY LAB G. REIO

NASA
GODDARO SPACE FLIGHT CENTER
GREENBELT, MD 20771
01CY ATTN P. CORRIGAN

OEPARTMENT OF OEFENSE CONTRACTORS

AEROSPACE CORPORATION
P. O. BOX 92957
LOS ANGELES, CA 90009
01CY ATTN I. GARFUNKEL
01CY ATTN T. SALMI
01CY ATTN V. JOSEPHSON
01CY ATTN S. BOWER
01CY ATTN N. STOCKWELL
01CY ATTN O. OLSEN
01CY ATTN J. CARTER
01CY ATTN F. MORSE
01CY ATTN SMFA FOR PWW

ANALYTICAL SYSTEMS ENGINEERING CORP
5 OLO CONCORO ROAD
BURLINGTON, MA 01803
01CY ATTN RAOIO SCIENCES

BERKELEY RESEARCH ASSOCIATES, INC.
P. O. BOX 983
BERKELEY, CA 94701
01CY ATTN J. WORKMAN

BOEING COMPANY, THE
P. O. BOX 3707
SEATTLE, WA 98124
01CY ATTN G. KEISTER
01CY ATTN O. MURRAY
01CY ATTN G. HALL
01CY ATTN J. KENNEY

CALIFORNIA AT SAN OIEGO, UNIV OF
IPAPS, B-019
LA JOLLA, CA 92093
01CY ATTN HENRY G. BOOKER

BROWN ENGINEERING COMPANY, INC.
CUMMINGS RESEARCH PARK
HUNTSVILLE, AL 35807
01CY ATTN ROMEO A. OELIBERIS

CHARLES STARK DRAPER LABORATORY, INC.
555 TECHNOLOGY SQUARE
CAMBRIDGE, MA 02139
01CY ATTN O. B. COX
01CY ATTN J. P. GILMORE

COMPUTER SCIENCES CORPORATION
6565 ARLINGTON BLVD
FALLS CHURCH, VA 22046
01CY ATTN H. BLANK
01CY ATTN JOHN SPOOR
01CY ATTN C. NAIL

COMSAT LABORATORIES
LINTHICUM ROAD
CLARKSBURG, MD 20734
01CY ATTN G. HYOE

CORNELL UNIVERSITY
DEPARTMENT OF ELECTRICAL ENGINEERING
ITHACA, NY 14850
01CY ATTN O. T. FARLEY JR

ELECTROSPACE SYSTEMS, INC.
BOX 1359
RICHARDSON, TX 75080
01CY ATTN H. LOGSTON
01CY ATTN SECURITY (PAUL PHILLIPS)

ESL INC.
495 JAVA DRIVE
SUNNYVALE, CA 94086
01CY ATTN J. ROBERTS
01CY ATTN JAMES MARSHALL
01CY ATTN C. W. PRETTIE

FORD AEROSPACE & COMMUNICATIONS CORP
3939 FABIAN WAY
PALO ALTO, CA 94303
01CY ATTN J. T. MATTINGLEY

GENERAL ELECTRIC COMPANY
SPACE DIVISION
VALLEY FORGE SPACE CENTER
GODDARO BLVD KING OF PRUSSIA
P. O. BOX 8555
PHILADELPHIA, PA 19101
01CY ATTN M. H. BORTNER SPACE SCI LAB

GENERAL ELECTRIC COMPANY
P. O. BOX 1122
SYRACUSE, NY 13201
01CY ATTN F. REIBERT

GENERAL ELECTRIC COMPANY
TEMPO-CENTER FOR ADVANCEO STUOIES
816 STATE STREET (P.O. DRAWER QQ)
SANTA BARBARA, CA 93102
01CY ATTN OASIAC
01CY ATTN DON CHANDLER
01CY ATTN TOM BARRETT
01CY ATTN TIM STEPHANS
01CY ATTN WARREN S. KNAPP
01CY ATTN WILLIAM MCNAMARA
01CY ATTN B. GAMBILL
01CY ATTN MACK STANTON

GENERAL ELECTRIC TECH SERVICES CO., INC.
HMES
COURT STREET
SYRACUSE, NY 13201
01CY ATTN G. MILLMAN

GENERAL RESEARCH CORPORATION
SANTA BARBARA OIVISION
P. O. BOX 6770
SANTA BARBARA, CA 93111
01CY ATTN JOHN ISE JR
01CY ATTN JOEL GARBARINO

GEOPHYSICAL INSTITUTE
UNIVERSITY OF ALASKA
FAIRBANKS, AK 99701
(ALL CLASS ATTN: SECURITY OFFICER)
01CY ATTN T. N. OAVIS (UNCL ONLY)
01CY ATTN NEAL BROWN (UNCL ONLY)
01CY ATTN TECHNICAL LIBRARY

GTE SYLVANIA, INC.
ELECTRONICS SYSTEMS GRP-EASTERN OIV
77 A STREET
NEEDHAM, MA 02194
01CY ATTN MARSHAL CROSS

ILLINOIS, UNIVERSITY OF
DEPARTMENT OF ELECTRICAL ENGINEERING
URBANA, IL 61803
01CY ATTN K. YEH

ILLINOIS, UNIVERSITY OF
107 COBLE HALL
801 S. WRIGHT STREET
URBANA, IL 60680
(ALL CORRES ATTN SECURITY SUPERVISOR FOR)
01CY ATTN K. YEH

INSTITUTE FOR DEFENSE ANALYSES
400 ARMY-NAVY ORIVE
ARLINGTON, VA 22202
01CY ATTN J. M. AEIN
01CY ATTN ERNEST BAUER
01CY ATTN HANS WOLFHARO
01CY ATTN JOEL BENGSTON

HSS, INC.
2 ALFREO CIRCLE
BEDFORD, MA 01730
01CY ATTN DONALO HANSEN

INTL TEL & TELEGRAPH CORPORATION
500 WASHINGTON AVENUE
NUTLEY, NJ 07110
01CY ATTN TECHNICAL LIBRARY

JAYCOR
1401 CAMINO DEL MAR
OEL MAR, CA 92014
01CY ATTN S. R. GOLDMAN

JOHNS HOPKINS UNIVERSITY
APPLIED PHYSICS LABORATORY
JOHNS HOPKINS ROAD
LAUREL, MD 20810
01CY ATTN DOCUMENT LIBRARIAN
01CY ATTN THOMAS PDTEMRA
01CY ATTN JOHN DASSOULAS

LOCKHEED MISSILES & SPACE CO INC
P. O. BOX 504
SUNNYVALE, CA 94088
01CY ATTN DEPT 60-12
01CY ATTN D. R. CHURCHILL

LOCKHEED MISSILES AND SPACE CO INC
3251 HANOVER STREET
PALO ALTO, CA 94304
01CY ATTN MARTIN WALT DEPT 52-10
01CY ATTN RICHARD G. JOHNSON DEPT 52-12
01CY ATTN W. L. IMHOF DEPT 52-12

KAMAN SCIENCES CORP
P. O. BOX 7463
COLORADO SPRINGS, CO 80933
01CY ATTN T. MEAGHER

LINKABIT CORP
10453 ROSELLE
SAN DIEGO, CA 92121
01CY ATTN IRWIN JACOBS

LOWELL RSCH FOUNDATION, UNIVERSITY OF
450 AIKEN STREET
LOWELL, MA 01854
01CY ATTN K. BIBL

M.I.T. LINCOLN LABORATORY
P. O. BOX 73
LEXINGTON, MA 02173
01CY ATTN DAVID M. TOWLE
01CY ATTN P. WALDRON
01CY ATTN L. LOUGHLIN
01CY ATTN D. CLARK

MARTIN MARIETTA CORP
ORLANDO DIVISION
P. O. BOX 5837
ORLANDO, FL 32805
01CY ATTN R. HEFFNER

MCDONNELL DOUGLAS CORPORATION
5301 BOLSA AVENUE
HUNTINGTON BEACH, CA 92647
01CY ATTN N. HARRIS
01CY ATTN J. MOULE
01CY ATTN GEORGE MROZ
01CY ATTN W. OLSON
01CY ATTN R. W. HALPRIN
01CY ATTN TECHNICAL LIBRARY SERVICES

MISSION RESEARCH CORPORATION
735 STATE STREET
SANTA BARBARA, CA 93101
01CY ATTN P. FISCHER
01CY ATTN W. F. CREVIER
01CY ATTN STEVEN L. GUTSCHE
01CY ATTN D. SAPPENFIELD
01CY ATTN R. BOGUSCH
01CY ATTN R. HENDRICK
01CY ATTN RALPH KILB
01CY ATTN DAVE SOWLE
01CY ATTN F. FAJEN
01CY ATTN M. SCHEIBE
01CY ATTN CONRAD L. LONGMIRE
01CY ATTN WARREN A. SCHLUETER

MITRE CORPORATION, THE
P. O. BOX 208
BEDFORD, MA 01730
01CY ATTN JOHN MORGANSTERN
01CY ATTN G. HARDING
01CY ATTN C. E. CALLAHAN

MITRE CORP
WESTGATE RESEARCH PARK
1820 OOLLY MADISON BLVD
MCLEAN, VA 22101
01CY ATTN W. HALL
01CY ATTN W. FOSTER

PACIFIC-SIERRA RESEARCH CORP
1456 CLOVERFIELD BLVD.
SANTA MONICA, CA 90404
01CY ATTN E. C. FIELD JR

PENNSYLVANIA STATE UNIVERSITY
IONOSPHERE RESEARCH LAB
318 ELECTRICAL ENGINEERING EAST
UNIVERSITY PARK, PA 16802
(NO CLASSIFIED TO THIS ADORESS)
01CY ATTN IONOSPHERIC RESEARCH LAB

PHOTOMETRICS, INC.
442 MARRETT ROAD
LEXINGTON, MA 02173
01CY ATTN IRVING L. KOFSKY

PHYSICAL DYNAMICS INC.
P. O. BOX 3027
BELLEVUE, WA 98009
01CY ATTN E. J. FREMOUW

PHYSICAL DYNAMICS INC.
P. O. BOX 1069
BERKELEY, CA 94701
01CY ATTN A. THOMPSON

R & O ASSOCIATES
P. O. BOX 9695
MARINA DEL REY, CA 90291
01CY ATTN FORREST GILMORE
01CY ATTN BRYAN GABBARD
01CY ATTN WILLIAM B. WRIGHT JR
01CY ATTN ROBERT F. LELEVIER
01CY ATTN WILLIAM J. KARZAS
01CY ATTN H. ORY
01CY ATTN C. MACDONALD
01CY ATTN R. TURCO

RAND CORPORATION, THE
1700 MAIN STREET
SANTA MONICA, CA 90406
01CY ATTN CULLEN CRAIN
01CY ATTN ED BEDROZIAN

RIVERSIDE RESEARCH INSTITUTE
80 WEST END AVENUE
NEW YORK, NY 10023
01CY ATTN VINCE TRAPANI

SCIENCE APPLICATIONS, INC.
P. O. BOX 2351
LA JOLLA, CA 92038
01CY ATTN LEWIS M. LINSON
01CY ATTN DANIEL A. HAMLIN
01CY ATTN D. SACHS
01CY ATTN E. A. STRAKER
01CY ATTN CURTIS A. SMITH
01CY ATTN JACK MCDOUGALL

RAYTHEON CO.
528 BOSTON POST ROAD
SUDBURY, MA 01776
01CY ATTN BARBARA ADAMS

SCIENCE APPLICATIONS, INC.
HUNTSVILLE DIVISION
2109 W. CLINTON AVENUE
SUITE 700
HUNTSVILLE, AL 35805
01CY ATTN DALE H. DIVIS

SCIENCE APPLICATIONS, INCORPORATED
8400 WESTPARK DRIVE
MCLEAN, VA 22101
01CY ATTN J. COCKAYNE

SCIENCE APPLICATIONS, INC.
80 MISSION DRIVE
PLEASANTON, CA 94566
01CY ATTN SZ

SRI INTERNATIONAL
333 RAVENSWOOD AVENUE
MENLO PARK, CA 94025
01CY ATTN DONALD NEILSON
01CY ATTN ALAN BURNS
01CY ATTN G. SMITH
01CY ATTN L. L. COBB
01CY ATTN DAVID A. JOHNSON
01CY ATTN WALTER G. CHESNUT
01CY ATTN CHARLES L. RINO
01CY ATTN WALTER JAYE
01CY ATTN M. BARON
01CY ATTN RAY L. LEADABRAND
01CY ATTN G. CARPENTER
01CY ATTN G. PRICE
01CY ATTN J. PETERSON
01CY ATTN R. HAKE, JR.
01CY ATTN V. GONZALES
01CY ATTN D. MCDANIEL

TECHNOLOGY INTERNATIONAL CORP
75 WIGGINS AVENUE
BEDFORD, MA 01730
01CY ATTN W. P. BOQUIST

TRW DEFENSE & SPACE SYS GROUP
ONE SPACE PARK
REDONDO BEACH, CA 90278
01CY ATTN R. K. PLEBUCH
01CY ATTN S. ALTSCHULER
01CY ATTN O. OEE

VISIONE, INC.
19 THIRD AVENUE
NORTH WEST INDUSTRIAL PARK
BURLINGTON, MA 01803
01CY ATTN CHARLES HUMPHREY
01CY ATTN J. W. CARPENTER